Analysis of the Power Coupling from a Waveguide Hyperthermia Applicator into a Three-Layered Tissue Model

KONSTANTINA S. NIKITA AND NIKOLAOS K. UZUNOGLU, MEMBER, IEEE

Abstract—**The power deposition from a rectangular-aperture flanged waveguide into a three-layered stratified tissue medium is analyzed theoretically. The fields inside the tissue layers are expressed in terms of Fourier integrals satisfying the corresponding wave equations while the fields inside the waveguide are expanded in terms of the guided and evanescent normal modes. An integral equation is derived on the aperture plane of the flanged waveguide by applying the continuity of the tangential electric and magnetic fields. This integral equation is solved by expressing the unknown electric field in terms of the waveguide mode fields and by applying a Galerkin procedure. The electromagnetic fields inside the tissue medium are then determined and patterns of the deposited power at frequencies of 432 MHz and 144 MHz for apertures of 5.6×2.8 cm^2 and 16.5×8.3 cm^2 respectively are computed and presented.**

I. Introduction

A WIDE VARIETY of hyperthermia applicators have been developed and used on an experimental basis in recent years [1]. Several authors have proposed the use of open-aperture waveguide applicators placed in contact with the tissue medium to be heated [2]–[4]. Dielectric loading of the waveguides usually is employed to effectively couple radiation into the tissue and to decrease the dimensions of the radiating apertures. In most cases pure water is used as a loading material.

The radiation from flanged rectangular open-aperture waveguides looking into free space has been considered by several authors in the past [5], [6]. The case of radiating apertures into a stratified medium has also been considered [7], [8]. The absorbed power distributions from single or multiple microwave waveguide applicators have been treated recently by Antolini *et al.* [9] employing a numerical solution of the coupled integral equations based on the method of moments. In this treatment power deposition patterns are presented for an unloaded waveguide with an aperture area of 130×100 mm^2 into a homogeneous tissue medium covered with a water bolus layer placed between the applicator aperture and the tissue medium.

In this paper the radiation from a water-loaded waveguide into a three-layered medium is treated semianalytically. The motivation of pursuing this work is the practical use of water-loaded waveguide applicators in hyperthermia, as described recently by Uzunoglu *et al.* [4]. The use of water loading provides several benefits, such as

a) the effective coupling of radiation into tissues;
b) a simple way of achieving low standing waves;
c) the elimination of the necessity of using cooling water bolus between the applicator and the skin;
d) the possibility of using a multiapplicator system because of the small aperture area of each applicator.

The recently gathered clinical experience in using 432 MHz water-loaded waveguide applicators (5.6×2.8 cm^2 aperture area) for superficial tumors substantiated the above points, and the development of a phased array system provided the rationale for analyzing in detail the behavior of this type of applicator at 432 MHz. The necessity of avoiding strong electric components normal to the fat layer, which can cause excessive heating of superficial layers, was also one of the reasons for treating this boundary value problem analytically [13]. In case of widespread tumors it is possible to employ several 432 MHz applicators and this has proved to be a good technique for heating superficial (less than 2.5 cm in depth) tumors covering an area wider than 3×4 cm^2. Furthermore in order to investigate the possibility of obtaining higher penetration depth the case of a 144 MHz water-loaded applicator has also been considered.

In the following analysis an $\exp(+j\omega t)$ time dependence is assumed for the field quantities and it is suppressed throughout the analysis.

II. Formulation of the Boundary Value Problem

The geometry of the rectangular waveguide applicator looking into a three-layered medium is shown in Fig. 1. The three layers correspond to skin, fat, and muscle (high water content) tissues. The rectangular waveguide aperture is assumed to be in direct contact with the skin surface. The electromagnetic properties of the layers are denoted with the corresponding relative complex permittivities ϵ_1, ϵ_2, and ϵ_3, as shown in Fig. 1. The analysis is pursued also by taking arbitrary relative magnetic permeabilities μ_1, μ_2, and μ_3, although in practice in tissue media $\mu_1=\mu_2=\mu_3$

Manuscript received February 21, 1989; revised May 30, 1989.
The authors are with the Department of Electrical Engineering, National Technical University of Athens, Athens 10682, Greece.
IEEE Log Number 8930518.

0018-9480/89/1100-1794$01.00

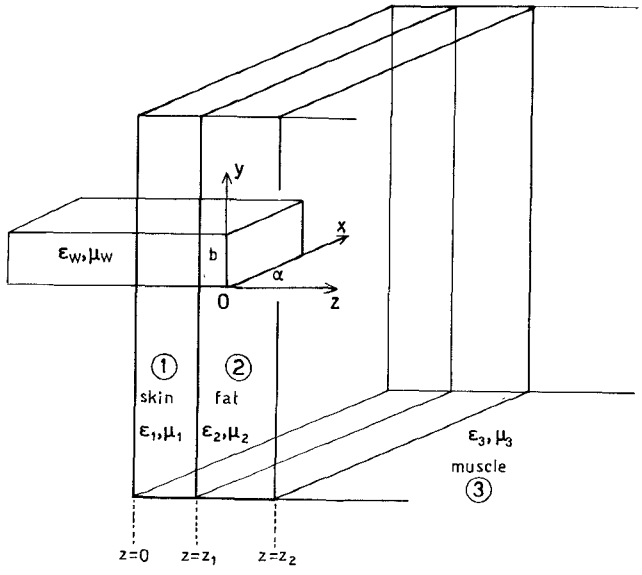

Fig. 1. Three-layered tissue model heated by a waveguide applicator with an infinite conductive flange.

$=1$. The free-space wavenumber is $k_0 = \omega\sqrt{\epsilon_0\mu_0}$, where ϵ_0 and μ_0 are the free-space permittivity and permeability, respectively. The rectangular waveguide is assumed to be filled with a dielectric material of relative permittivity ϵ_w and relative permeability μ_w. In order to have a tractable solution, an infinitely large conductive flange at $z = 0$ is assumed.

A. Electromagnetic Fields Inside the Tissue Layers

The assumption of a stratified tissue model invokes the use of Fourier integrals to express the solution of the wave equation:

$$\left(\nabla \times \nabla \times - k_0^2 \epsilon_i \mu_i\right) \boldsymbol{E}_i(\boldsymbol{r}) = 0 \tag{1}$$

where $i = 1,2,3$ corresponds to the three regions. Then,

$$\boldsymbol{E}_i(\boldsymbol{r}) = \int_{-\infty}^{+\infty} d\alpha \int_{-\infty}^{+\infty} d\beta\, e^{j(\alpha x + \beta y)} \left(\boldsymbol{A}_i e^{-\gamma_i z} + \boldsymbol{A}_i' e^{\gamma_i z}\right) \tag{2}$$

where the x, y, and z rectangular coordinates are shown in Fig. 1,

$$\gamma_i = \left(\alpha^2 + \beta^2 - k_0^2 \epsilon_i \mu_i\right)^{1/2} \tag{3}$$

and $\boldsymbol{A}_i$ and $\boldsymbol{A}_i'$ are unknown vector coefficients to be determined. According to Gauss's theorem, inside the ith layer,

$$\nabla \cdot \boldsymbol{E}_i(\boldsymbol{r}) = 0 \tag{4}$$

and then

$$\boldsymbol{A}_i \cdot (j\boldsymbol{\lambda} - \gamma_i \hat{z}) = 0 \qquad \boldsymbol{A}_i' \cdot (j\boldsymbol{\lambda} + \gamma_i \hat{z}) = 0 \tag{5}$$

where $\boldsymbol{\lambda} = \alpha\hat{x} + \beta\hat{y}$ should be satisfied for $i = 1$, 2, and 3. By using (5), the z components (A_{iz}, A_{iz}') of the $\boldsymbol{A}_i$ and $\boldsymbol{A}_i'$ vectors can be expressed in terms of the transversal (A_{ix}, A_{iy}) and (A_{ix}', A_{iy}') components, and on substituting these terms into (2) the following electric field expression is derived:

$$\boldsymbol{E}_i(\boldsymbol{r}) = \int_{-\infty}^{+\infty} \int_{-\infty}^{+\infty} d\alpha\, d\beta \left[e^{-\gamma_i z}\left(A_{xi}\boldsymbol{\chi}_i + A_{yi}\boldsymbol{\psi}_i\right) + e^{\gamma_i z}\left(A_{xi}'\boldsymbol{\chi}_i' + A_{yi}'\boldsymbol{\psi}_i'\right)\right] e^{j\boldsymbol{\lambda}\cdot\boldsymbol{r}} \tag{6}$$

where

$$\boldsymbol{r} = x\hat{x} + y\hat{y} + z\hat{z}$$

$$\boldsymbol{\chi}_i = \hat{x} + j\frac{\alpha}{\gamma_i}\hat{z} \tag{7a}$$

$$\boldsymbol{\psi}_i = \hat{y} + j\frac{\beta}{\gamma_i}\hat{z} \tag{7b}$$

$$\boldsymbol{\chi}_i' = \hat{x} - j\frac{\alpha}{\gamma_i}\hat{z} \tag{7c}$$

$$\boldsymbol{\psi}_i' = \hat{y} - j\frac{\beta}{\gamma_i}\hat{z} \tag{7d}$$

and $i = 1,2,3$.

The corresponding magnetic field inside the ith layer can be computed easily by employing the Maxwell–Faraday equation, leading to the expression

$$\boldsymbol{H}_i(\boldsymbol{r}) = \frac{j}{\omega\mu_0\mu_i} \int_{-\infty}^{+\infty} \int_{-\infty}^{+\infty} d\alpha\, d\beta \left[e^{-\gamma_i z}\left(A_{xi}\boldsymbol{\tau}_i + A_{yi}\boldsymbol{\zeta}_i\right) + e^{\gamma_i z}\left(A_{xi}'\boldsymbol{\tau}_i' + A_{yi}'\boldsymbol{\zeta}_i'\right)\right] \tag{8}$$

where

$$\boldsymbol{\tau}_i = -\frac{\alpha\beta}{\gamma_i}\hat{x} + \frac{k_0^2\epsilon_i\mu_i - \beta^2}{\gamma_i}\hat{y} - j\beta\hat{z} \tag{9a}$$

$$\boldsymbol{\zeta}_i = -\frac{k_0^2\epsilon_i\mu_i - \alpha^2}{\gamma_i}\hat{x} + \frac{\alpha\beta}{\gamma_i}\hat{y} + j\alpha\hat{z} \tag{9b}$$

$$\boldsymbol{\tau}_i' = \frac{\alpha\beta}{\gamma_i}\hat{x} - \frac{k_0^2\epsilon_i\mu_i - \beta^2}{\gamma_i}\hat{y} - j\beta\hat{z} \tag{9c}$$

$$\boldsymbol{\zeta}_i' = -\frac{k_0^2\epsilon_i\mu_i - \alpha^2}{\gamma_i}\hat{x} - \frac{\alpha\beta}{\gamma_i}\hat{y} + j\alpha\hat{z} \tag{9d}$$

with $i = 1,2,3$.

Considering the semi-infinite extent of the $i = 3$ muscle tissue medium and because of the radiation (outgoing) wave conditions in (6) it is required that

$$A_{x3}' = A_{y3}' = 0 \tag{10}$$

subject to the conditions

$$\mathrm{Re}(\gamma_e) > 0 \qquad \mathrm{Im}(\gamma_3) > 0. \tag{11}$$

Inside the $i = 1$ and 2 (skin and fat) layers, respectively, both $\exp(-\gamma_i z)$ and $\exp(\gamma_i z)$ solutions are encountered because of the standing wave character of the field distributions. On satisfying the continuity of the tangential (x and y) electric and magnetic field components on the $z = z_1$ (skin–fat) and $z = z_2$ (fat–muscle) planes, a system of two equations is obtained on each interface plane for x and y components independently. Then by eliminating the $A_{x3}(A_{y3})$ coefficient the "reflected" wave amplitudes

A'_{x2}, A'_{y2} can be expressed in terms of the "incident" A_{x2}, A_{y2} amplitudes. At the end of this procedure the following relation is obtained:

$$\boldsymbol{\alpha}'_2 = \bar{\boldsymbol{R}}_2 \cdot \boldsymbol{\alpha}_2 \tag{12}$$

where

$$\boldsymbol{\alpha}_2 = A_{x2}\hat{x} + A_{y2}\hat{y}$$

$$\boldsymbol{\alpha}'_2 = A'_{x2}\hat{x} + A'_{y2}\hat{y}$$

are transversal vector coefficients, and

$$\bar{\boldsymbol{R}}_2 = e^{-2\gamma_2 z_2}\left(\bar{\boldsymbol{D}}_3 + \bar{\boldsymbol{D}}_2\right)^{-1} \cdot \left(\bar{\boldsymbol{D}}_2 - \bar{\boldsymbol{D}}_3\right) \tag{13}$$

$$\bar{\boldsymbol{D}}_i = \begin{pmatrix} -\dfrac{\alpha\beta}{\gamma_i \mu_i} & -\dfrac{k_0^2 \epsilon_i \mu_i - \alpha^2}{\gamma_i \mu_i} \\ \dfrac{k_0^2 \epsilon_i \mu_i - \beta^2}{\gamma_i \mu_i} & \dfrac{\alpha\beta}{\gamma_i \mu_i} \end{pmatrix} \tag{14}$$

with $i = 2, 3$.

In the same manner by applying the boundary conditions on the $z = z_1$ (skin–fat) layers' interface and then eliminating the $\boldsymbol{\alpha}'_2, \boldsymbol{\alpha}_2$ coefficients, the following relation is obtained between the $\boldsymbol{\alpha}'_1$ and $\boldsymbol{\alpha}_1$ transverse vectors:

$$\boldsymbol{\alpha}'_1 = \bar{\boldsymbol{R}}_1 \cdot \boldsymbol{\alpha}_1 \tag{15}$$

where

$$\boldsymbol{\alpha}_1 = A_{x1}\hat{x} + A_{y1}\hat{y}$$

$$\boldsymbol{\alpha}'_1 = A'_{x1}\hat{x} + A'_{y1}\hat{y}$$

$$\bar{\boldsymbol{R}}_1 = -e^{-2\gamma_1 z_1}\left(\bar{\boldsymbol{D}}_1 + \bar{\boldsymbol{T}}_2 \cdot \bar{\boldsymbol{Q}}_2\right)^{-1}\left(\bar{\boldsymbol{T}}_2 \bar{\boldsymbol{Q}}_2 - \bar{\boldsymbol{D}}_1\right) \tag{16}$$

where $\bar{\boldsymbol{D}}_1$ is obtained by setting $i = 1$ in (16) and

$$\bar{\boldsymbol{T}}_2 = e^{-\gamma_2 z_1}\bar{\boldsymbol{D}}_2 - e^{\gamma_2 z_1}\bar{\boldsymbol{D}}_2 \cdot \bar{\boldsymbol{R}}_2 \tag{17}$$

$$\bar{\boldsymbol{Q}}_2 = \left(e^{-\gamma_2 z_1}\bar{\boldsymbol{I}} + e^{\gamma_2 z_1} \cdot \bar{\boldsymbol{R}}_2\right)^{-1} \tag{18}$$

with

$$\bar{\boldsymbol{I}} = \begin{pmatrix} 1 & 0 \\ 0 & 1 \end{pmatrix}$$

being the identity operator.

Substituting (17) into (2) for $i = 1$, the transverse electric field inside the skin layer is obtained in the following form:

$$\boldsymbol{E}_{1,t}(\boldsymbol{r}) = \int_{-\infty}^{+\infty} d\alpha \int_{-\infty}^{+\infty} d\beta \cdot e^{j(\alpha x + \beta y)} \bar{\boldsymbol{L}}(\alpha, \beta/z) \cdot \boldsymbol{\alpha}_1 \tag{19}$$

with $0 < z < z_1$ and

$$\bar{\boldsymbol{L}}(\alpha, \beta) = \left(e^{-\gamma_1 z}\bar{\boldsymbol{I}} + e^{\gamma_1 z}\bar{\boldsymbol{R}}_1\right). \tag{20}$$

The subscript t in (19) is to denote the transverse character of the electric field.

If the $\boldsymbol{\alpha}_1$ vector coefficient is known, then the electric field inside the tissue layers can be computed easily by using (19) and the vector relations between the $\boldsymbol{\alpha}_3$, $\boldsymbol{\alpha}_2$, $\boldsymbol{\alpha}'_2$, and $\boldsymbol{\alpha}_1$ coefficients.

B. Electromagnetic Fields Inside the Waveguide Applicator

The normal modes satisfying the boundary conditions on the sidewalls of the rectangular waveguide are very well known [10]. In order to achieve in practice a stable operation of the waveguide applicator and a good match to a power generator, it is desirable to have only a single propagating mode. This means that only the TE_{10} mode cutoff frequency should be less than the operating frequency. There are an infinite number of evanescent modes. These modes are present only near the discontinuity regions, such as the open aperture of the rectangular waveguide (see Fig. 1). Therefore the fields inside the waveguide can be described as the superposition of the incident TE_{10} mode and an infinite sum of all the reflected modes. Following the notation of [10], the transverse electric field inside the waveguide can be written as follows:

$$\boldsymbol{E}_{w,t}(\boldsymbol{r}) = \boldsymbol{e}^{\mathrm{TE}}_{1,t}(x, y)\frac{j\omega\mu_0\mu_w}{u_m}e^{-jk_m z} + \sum_{m=1}^{\infty}\left(A'_m \boldsymbol{e}^{\mathrm{TE}}_{m,t}(x, y)\frac{j\omega\mu_0\mu_w}{u_m}e^{jk_m z} + B'_m \boldsymbol{e}^{\mathrm{TM}}_{m,t}(x, y)\cdot\left(-\frac{j\lambda_m}{v_m}\right)e^{j\lambda_m z}\right) \tag{21}$$

where the subscript t is used to denote the transverse field components, and k_m and λ_m are propagation constants of TE and TM modes, respectively:

$$\lambda_m = \sqrt{k_0^2 \epsilon_w \mu_w - v_m^2} \tag{22a}$$

$$k_m = \sqrt{k_0^2 \epsilon_w \mu_w - u_m^2} \tag{22b}$$

The transverse $\boldsymbol{e}^{\mathrm{TE}}_{m,t}$ and $\boldsymbol{e}^{\mathrm{TM}}_{m,t}$ modal fields are [10]

$$\boldsymbol{e}^{\mathrm{TE}}_{m,t} = (\hat{z}x\nabla_t\psi_m)/u_m \qquad \boldsymbol{e}^{\mathrm{TM}}_{m,t} = \nabla_t\varphi_m/v_m \tag{23}$$

with $\nabla_t = (\partial/\partial x\hat{x} + \partial/\partial y\hat{y})$. The scalar functions ψ_m and φ_m satisfy the wave equations

$$\left(\nabla^2 + u_m^2\right)\psi_m = 0 \qquad \left(\nabla^2 + v_m^2\right)\varphi_m = 0 \tag{24}$$

and the boundary conditions

$$\partial\psi_m/\partial n = 0 \qquad \varphi_m = 0 \tag{25}$$

on the walls of the waveguide, with $\partial/\partial n$ being the normal derivative.

Furthermore by scaling appropriately the $\boldsymbol{e}^{\mathrm{TE}}_{m,t}$ and $\boldsymbol{e}^{\mathrm{TM}}_{m,t}$ vectors and taking advantage of their orthogonality, it can be shown that [10]

$$\iint \boldsymbol{e}^{\mathrm{TE}}_{m,t} \cdot \boldsymbol{e}^{\mathrm{TE}}_{p,t}\, dx\, dy = \iint \boldsymbol{e}^{\mathrm{TM}}_{m,t} \cdot \boldsymbol{e}^{\mathrm{TM}}_{p,t}\, dx\, dy = \delta_{pm} \tag{26}$$

$$\iint \boldsymbol{e}^{\mathrm{TE}}_{m,t} \cdot \boldsymbol{e}^{\mathrm{TM}}_{p,t}\, dx\, dy = 0 \tag{27}$$

where the integrals are computed on an arbitrary cross section of the waveguide, and δ_{pm} is the Kronecker delta.

The magnetic fields associated with the $\boldsymbol{e}^{\mathrm{TE}}_{m,t}$ and $\boldsymbol{e}^{\mathrm{TM}}_{m,t}$ fields can be written as follows [10]:

$$\boldsymbol{h}^{\mathrm{TE}}_{m,t} = -\frac{1}{u_m}\nabla_t\psi_m \qquad \boldsymbol{h}^{\mathrm{TM}}_{m,t} = \frac{1}{v_m}\hat{z}x\nabla_t\varphi_m. \tag{28}$$

The magnetic field corresponding to the electric field of (21) can be derived by again employing the Maxwell–Faraday equation.

C. Integral Equation on the $z = 0$ Aperture Plane

In order to satisfy the continuity of the electric and magnetic fields on the $z = 0$ aperture plane, an unknown transverse aperture field $\boldsymbol{E}_\alpha(x, y)$ is defined. Then on the $z = 0$ infinite plane it is required that

$$\boldsymbol{E}_\alpha(x, y) = \begin{cases} 0 & \text{outside the aperture} \\ \boldsymbol{E}_{w,t}(x, y, z = 0) \end{cases} \tag{29}$$

and

$$\boldsymbol{E}_\alpha(x, y) = \boldsymbol{E}_{1,t}(x, y, z = 0). \tag{30}$$

Notice that the $\boldsymbol{E}_{1,t}$ and $\boldsymbol{E}_{w,t}$ fields have already been expressed in (19) and (21), respectively, in terms of unknown coefficients α_1, A'_m, and B'_m. These coefficients can be expressed in terms of the aperture function $\boldsymbol{E}_\alpha(x, y)$, which is also an unknown quantity. To this end the orthogonality of Fourier integrals and the relations given in (26) and (27) are employed to obtain the expressions

$$\alpha_1(\alpha, \beta) = \frac{\left(\bar{L}(\alpha, \beta, 0)\right)^{-1}}{(2\pi)^2} \iint_{\text{aperture}} dx\,dy\,\boldsymbol{E}_\alpha(x, y) e^{-j\alpha x - j\beta y} \tag{31}$$

$$\delta_{m1} + A'_m = \frac{u_m}{j\omega\mu_0\mu_w} \iint_{\text{aperture}} dx\,dy\,\boldsymbol{E}_\alpha(x, y) \cdot \boldsymbol{e}^{\text{TE}}_{m,t}(x, y) \tag{32}$$

$$B'_m = -\frac{v_m}{j\lambda_m} \iint_{\text{aperture}} dx\,dy\,\boldsymbol{E}_\alpha(x, y) \cdot \boldsymbol{e}^{\text{TM}}_{m,t}(x, y). \tag{33}$$

The final step in obtaining the fundamental integral equation is to satisfy the continuity of the tangential magnetic fields on the $z = 0$ plane. By substituting (31), (32), and (33) into this boundary condition and using the Fourier integral convolution theorem, after a lengthy but otherwise straightforward algebra the following integral equation is obtained:

$$\iint_{\text{aperture}} dx'\,dy'\,\bar{\boldsymbol{K}}(x, y/x', y') \cdot \boldsymbol{E}_\alpha(x', y') = 2\boldsymbol{h}^{\text{TE}}_{1,t}(x, y)\left(\frac{jk_1}{u_1}\right) \tag{34}$$

where

$$\boldsymbol{h}^{\text{TE}}_{1,t} = -\frac{1}{u_1}\nabla_t\psi_1 \tag{35}$$

is the incident TE_{10} mode transverse magnetic field, and the kernel matrix function $\bar{\boldsymbol{K}}(x, y/x', y')$ is given in the Appendix.

III. Solution of the Integral Equation

In order to determine the electric fields inside the tissue layers and the waveguide region (mainly the reflected TE_{10} mode amplitude) the integral equation (34) was solved. To this end a Galerkin's technique is adopted by expanding the $\boldsymbol{E}_\alpha$ transverse aperture electric field into waveguide normal modes:

$$\boldsymbol{E}_\alpha = \sum_{m=1}^{\infty} \left(g_m \boldsymbol{e}^{\text{TE}}_{m,t} + p_m \boldsymbol{e}^{\text{TM}}_{m,t}\right). \tag{36}$$

By substituting (36) into (34), taking the inner products of both sides with $\boldsymbol{h}^{\text{TE}}_{n,t}$ and $\boldsymbol{h}^{\text{TM}}_{n,t}$, the magnetic vectors of the TE and TM modes, and then integrating over the waveguide aperture, the integral equation (34) is converted into an infinite system of linear equations of the following type:

$$\sum_{m=1}^{\infty} \begin{pmatrix} K^{EE}_{nm} & K^{EM}_{nm} \\ K^{ME}_{nm} & K^{MM}_{nm} \end{pmatrix} \cdot \begin{pmatrix} g_m \\ p_m \end{pmatrix} = \begin{pmatrix} 2jk_1/u_1 \\ 0 \end{pmatrix} \tag{37}$$

where

$$\begin{bmatrix} K^{EE}_{nm} \\ K^{EM}_{nm} \\ K^{ME}_{nm} \\ K^{MM}_{nm} \end{bmatrix} = \iint_{\text{aperture}} dx\,dy \iint_{\text{aperture}} dx'\,dy' \begin{bmatrix} \boldsymbol{h}^{\text{TE}}_{n,t}(x, y) \\ \boldsymbol{h}^{\text{TE}}_{n,t}(x, y) \\ \boldsymbol{h}^{\text{TM}}_{n,t}(x, y) \\ \boldsymbol{h}^{\text{TM}}_{n,t}(x, y) \end{bmatrix} \cdot \bar{\boldsymbol{K}} \cdot \begin{bmatrix} \boldsymbol{e}^{\text{TE}}_{m,t}(x', y') \\ \boldsymbol{e}^{\text{TM}}_{m,t}(x', y') \\ \boldsymbol{e}^{\text{TE}}_{m,t}(x', y') \\ \boldsymbol{e}^{\text{TM}}_{m,t}(x', y') \end{bmatrix}. \tag{38}$$

In computing the numerical values of the matrix elements K^{EE}_{nm}, K^{EM}_{nm}, K^{ME}_{nm}, and K^{MM}_{nm}, the expression for the $\bar{\boldsymbol{K}}$ matrix given in the Appendix is employed. Diagonal matrix elements ($m = n$) are obtained due to the waveguide mode contributions to the $\bar{\boldsymbol{K}}$ matrix. Concerning the stratified layer contribution to $\bar{\boldsymbol{K}}$, the Fourier transformations of $\boldsymbol{h}^{\text{TE}}_{n,t}$, $\boldsymbol{h}^{\text{TM}}_{n,t}$ and $\boldsymbol{e}^{\text{TE}}_{m,t}$, $\boldsymbol{e}^{\text{TM}}_{m,t}$ on the applicator aperture are encountered, which are computed easily. Then a double infinite inverse Fourier integral transformation is obtained. This integral is computed by applying a Gauss rule integration algorithm. A sufficient number of integration points are taken to ensure accuracy. Furthermore the bounds of the integrals are truncated as high as $\alpha, (\beta) \sim 60k_0$ to attain good convergence.

Assuming the g_m and p_m expansion coefficients are determined approximately, the aperture field can be determined approximately by using (36). On substituting (36) into (31) and computing the Fourier transformations of the $\boldsymbol{e}^{\text{TE}}_{m,t}$ and $\boldsymbol{e}^{\text{TM}}_{m,t}$ modal fields, the $\alpha_1(\alpha, \beta)$ vector coefficient is determined easily. Then by employing the reflection matrix relations given in (15) and (12) and the continuity conditions of the transverse electric fields on the $z = z_1$ and $z = z_2$ interface planes, the vector coefficients α_2, α'_2, α_3, and α'_3 are determined. Substituting the values of these vector coefficients into (6), the electric field is obtained in the form of an inverse Fourier integral.

IV. Numerical Results and Discussion

Numerical computations have been performed by applying the analysis method developed in the previous sections. In order to check the developed numerical code, several trials have been performed. In the first place the convergence and stability of the solution are examined by increasing the number of modes included in the aperture electric field $\boldsymbol{E}_\alpha$ (eq. (36)). Because of the x and y axes of symmetry, a subset of modes are excited on the applicator aperture and therefore also inside the waveguide. In Table I convergence patterns are presented in terms of the TE_{10} mode reflection coefficient and electric fields. The continuity of the tangential fields at the $z = z_1$ and $z = z_2$ interface planes has been checked and verified numerically. Furthermore, the validity of the boundary conditions on the $z = 0$ aperture plane has also been checked. In Fig. 2 the aperture electric field intensities computed directly from the series of (36) and by the Fourier integral of (19) when $z \to 0$ are compared. It is known that the Galerkin technique employed in Section III satisfies the boundary conditions on the $z = 0$ plane approximately. This is exhibited in Fig. 2. Notice that at the waveguide aperture edge the well-known Gibbs phenomenon [11] associated with Fourier series is observed.

Because of the integration procedure used in (6) to compute the electric field intensity at an arbitrary point in terms of the $\alpha_i(\alpha, \beta)$ and $\alpha_i'(\alpha, \beta)$ coefficients, the obtained solution is stationary.

This means that if the error in computing the aperture field is of $|\delta \boldsymbol{E}_\alpha|$ order, the computed electric field intensities at an arbitrary point are only of an $|\delta \boldsymbol{E}_\alpha|^2$ order in error. This fact is exhibited clearly in Table I, where the convergence patterns of the $\boldsymbol{E}_\alpha$ aperture field and of the electric field on the waveguide axis inside the muscle tissue are also presented.

The power deposition patterns at a frequency of 432 MHz for a water-loaded waveguide of 5.6×2.8 cm^2 have been computed and are presented in Fig. 3. Because of the x and y symmetry, only a single quadrant of the electric field $|\boldsymbol{E}_i|$ intensity distribution is presented on each $z =$ constant plane. The thicknesses of the skin and fat layers are taken to be

$$z_1 = 0.5 \text{ cm}$$

$$z_2 - z_1 = 1.0 \text{ cm}$$

and the corresponding complex relative permittivities, which are compiled from the relevant literature, are taken to be [12]

$$\epsilon_1 = \epsilon_3 = 42 - j25 \quad \text{(skin, muscle tissue)}$$

$$\epsilon_2 = 5 - j10 \quad \text{(fat tissue)}.$$

The permittivity of the water filling the waveguide is taken to be real and $\epsilon_w = 81$.

Notice that on the $z = z_1$ and $z = z_2$ planes, the longitudinal E_{iz} electric field components should present a discontinuity. Therefore the $|\boldsymbol{E}_i|$ intensities also exhibit discontinuity off the axis of the waveguide. On the waveguide axis the field intensity is purely transverse. It is known that the applicator field inside the tissue should as much as possible be transverse since longitudinal components give rise to overheating of the fat layers [13]. The intensity distribution inside the muscle tissue on a given $z =$ constant plane is relatively uniform within an area approximately equal to the applicator aperture. In practice the rather high power deposition into the skin layer is eliminated by cooling the skin surface by the applicator itself. Because of the small conductivity of the fat tissue, the deposited power is also very small. The longitudinal components appearing near the aperture edge are relatively small and are considered to be second-order phenomena not leading to overheating of the fat layer. Therefore the main heating occurs inside the muscle tissue in a region limited to a 1–1.5 cm penetration depth from the $z = z_2$ plane (see Fig. 1).

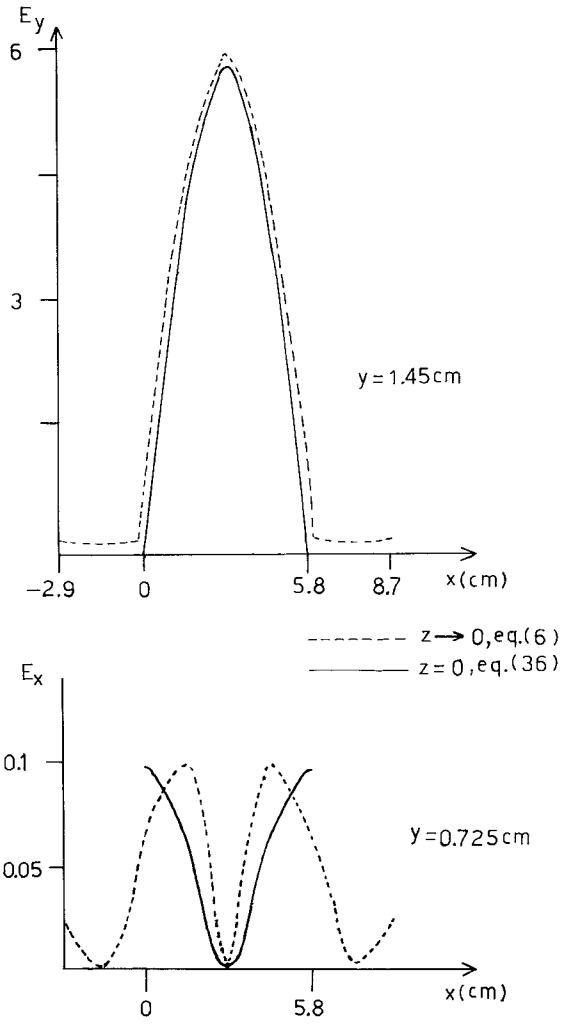

Fig. 2. Aperture field distributions at 432 MHz: comparison of the results of eqs. (36) and (6).

In order to achieve higher penetration depths and to cover wider areas with a single applicator, the possibility of employing a 144 MHz radiation frequency has been investigated. The waveguide applicator dimensions are ap-

TABLE I
CONVERGENCE FOR THE TE_{10} REFLECTION COEFFICIENT $\rho = A_1^r$ (SEE EQ. (21)) AND ELECTRIC FIELD INTENSITY AT THREE POINTS ON THE BORESIGHT AXIS BY INCREASING THE APERTURE MODE NUMBER

Modes included	ρ	$\lvert E_\alpha \rvert$ (V/m) x = 2.9 cm, y = 1.45cm, z = 0 cm	$\lvert E \rvert$ (V/m) x = 2.9 cm, y = 1.45cm, z = 1.5 cm	$\lvert E \rvert$ (V/m) x = 2.9 cm, y = 1.45cm, z = 2.5 cm
TE_{10}	$0.49475e^{j30^\circ}$	617	177	109
TE_{10} TE_{12} TM_{12}	$0.49695e^{j29^\circ}$	587	175	108
TE_{10} TE_{12} TE_{30} TE_{32} TM_{12} TM_{32}	$0.49391e^{j28.8^\circ}$	582	173.5	108

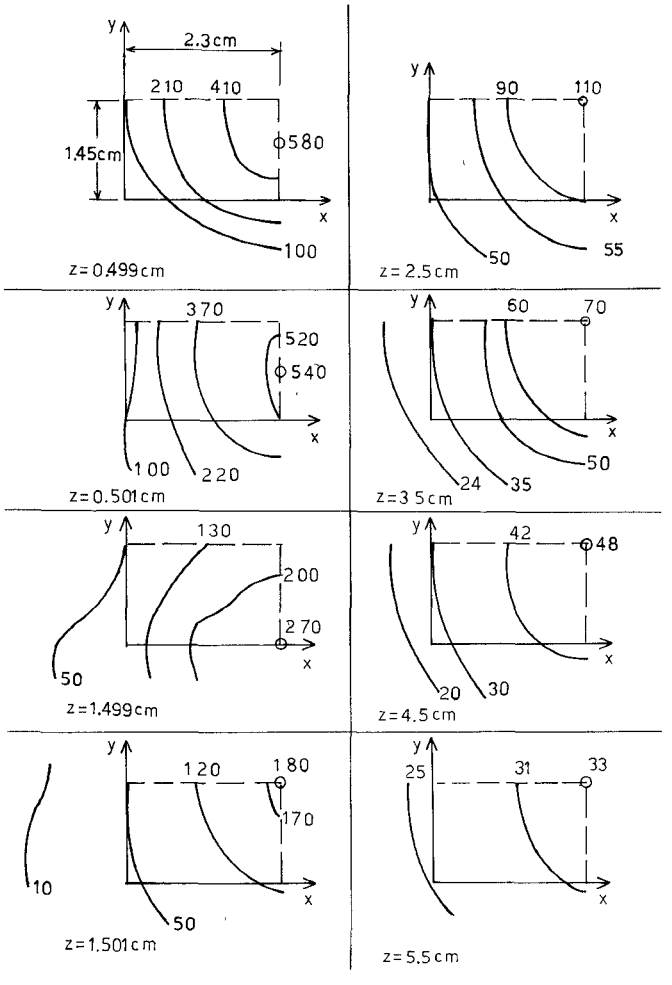

Fig. 3. Electric field intensity $|E|$ at several z = constant planes for the 432 MHz applicator and 1 W radiated power.

proximately three times larger than those of the 432 MHz applicator. The numerical results are presented in Fig. 4 in a form similar to those of the 432 MHz case. In this case the relative complex permittivities are taken to be

$$\epsilon_1 = \epsilon_3 = 65 - j115 \quad \text{(skin, muscle tissue)}$$

$$\epsilon_2 = 8 - j7 \quad \text{(fat tissue)}.$$

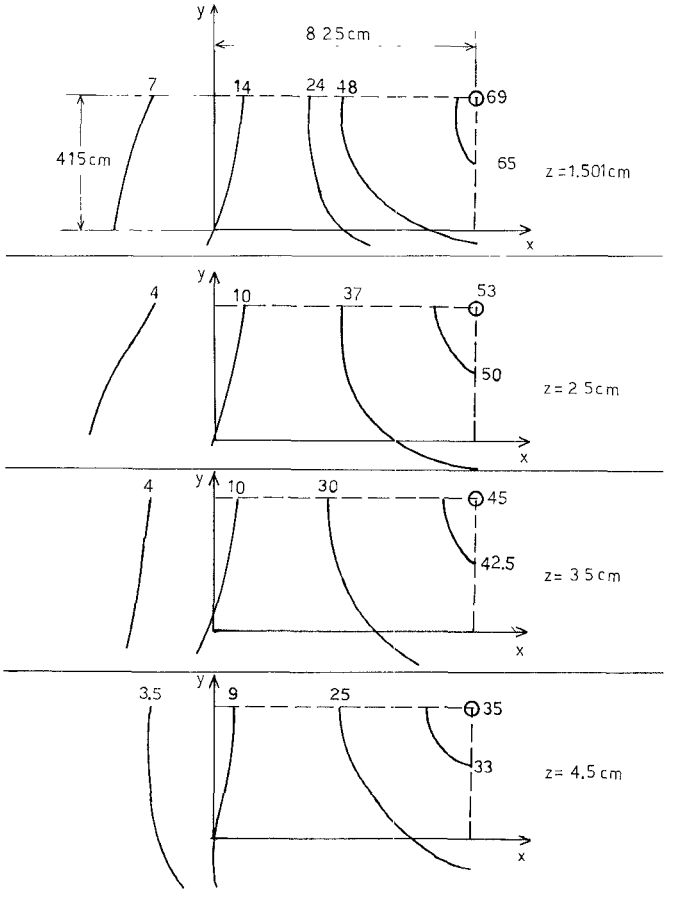

Fig. 4. Electric field intensity $|E|$ at several z = constant planes for the 144 MHz applicator and 1 W radiated power.

A pattern similar to the 432 MHz applicator is observed but the covered area is almost ten times larger and the half-power penetration depth is of the order of 2.5–3 cm.

Considering the requirement of achieving half-power penetration depths of the order of 5–8 cm, it is clear that this cannot be achieved with either of the applicators when they are used alone. It seems that there are two possible solutions: either employ an applicator operating at a lower radiation frequency or use several applicators by employing a phased array principle. The former solution has been already considered by developing ridge waveguide applicators operating at 27 MHz. However the half-power penetration depth is still limited to 4.5 cm. The latter approach has already been considered by several authors and a system operating at 50–110 MHz has been developed using 16 water-loaded TEM horn antennas [14], [15]. The focusing capability of this system has been shown experimentally. An alternative method is to employ TE_{10} waveguide applicators placed on the body surface at appropriate positions to achieve the best focusing. A four-applicator-element phased array hyperthermia system operating at 432 MHz has been developed and the analysis presented in this paper is being employed to compute the power patterns within the tissues. The performance of this system will be presented elsewhere.

It is important to emphasize that in the presented results all boundary conditions are satisfied on the tissue interface layers (exactly) and on the antenna aperture (approximately in a point matching sense). Considering also the fact that the field expressions satisfy Maxwell's equations, it is concluded that the developed solution and the presented results are self-consistent and accurate within the framework of the approximate solution of integral equation (34).

V. Conclusions

A semianalytical solution has been presented for the power coupling from a waveguide hyperthermia applicator into a three-layered tissue medium. Power deposition patterns of two practical waveguide applicators have been computed at 432 and 144 MHz. These results are useful in designing applicators and in analyzing the performance of phased array hyperthermia systems employing several applicators.

Appendix
Dyadic Kernel Function $\bar{K}(x, y/x', y')$

$$\bar{K}(x, y/x', y') = \int_{-\infty}^{+\infty} d\alpha \int_{-\infty}^{+\infty} d\beta \bar{N}(\alpha, \beta) - \bar{\Omega}(x, y/x', y') \tag{A1}$$

where

$$\bar{\Omega}(x, y/x', y') = \sum_{m=1}^{\infty} \left\{ \left(\frac{-k_m}{\omega \mu_0 \mu_w} \right) \boldsymbol{h}_{m,t}^{\mathrm{TE}} \boldsymbol{e}_{m,t}^{\mathrm{TE}} + \left(\frac{\omega \epsilon_0 \epsilon_w}{\lambda_m} \right) \boldsymbol{h}_{m,t}^{\mathrm{TM}} \boldsymbol{e}_{m,t}^{\mathrm{TM}} \right\} \tag{A2}$$

$$\bar{N}(\alpha, \beta) = \frac{j}{\omega \mu_0 \mu_1} \frac{1}{(2\pi)^2} \begin{pmatrix} \boldsymbol{F}'(\alpha,\beta)\cdot\hat{x} & \boldsymbol{G}'(\alpha,\beta)\cdot\hat{x} \\ \boldsymbol{F}'(\alpha,\beta)\cdot\hat{y} & \boldsymbol{G}'(\alpha,\beta)\cdot\hat{y} \end{pmatrix} \cdot \begin{pmatrix} \boldsymbol{F}(\alpha,\beta)\cdot\hat{x} & \boldsymbol{G}(\alpha,\beta)\cdot\hat{x} \\ \boldsymbol{F}(\alpha,\beta)\cdot\hat{y} & \boldsymbol{G}(\alpha,\beta)\cdot\hat{y} \end{pmatrix}^{-1} \tag{A3}$$

where

$$\boldsymbol{F}(\alpha, \beta) = \boldsymbol{x}_1 + R_1^{11} \boldsymbol{x}_1' + R_1^{21} \psi_1' \tag{A4}$$

$$\boldsymbol{G}(\alpha, \beta) = \psi_1 + R_1^{12} \boldsymbol{x}_1' + R_1^{22} \psi_1' \tag{A5}$$

$$\boldsymbol{F}'(\alpha, \beta) = \tau_1 + R_1^{11} \tau_1' + R_1^{21} \zeta_1' \tag{A6}$$

$$\boldsymbol{G}'(\alpha, \beta) = \zeta_1 + R_1^{12} \tau_1' + R_1^{22} \zeta_1' \tag{A7}$$

and R_1^{ij} $(i=1,2;\ j=1,2)$ are the elements of the reflection matrix $\bar{\boldsymbol{R}}_1$ defined in (16) and

$$\bar{\boldsymbol{R}}_1 = \begin{pmatrix} R_1^{11} & R_1^{12} \\ R_1^{21} & R_1^{22} \end{pmatrix}. \tag{A8}$$

References

[1] J. W. Strohbehn and E. B. Douple, "Hyperthermia and cancer therapy: A review of biomedical engineering contributions and challenges," *IEEE Trans. Biomed. Eng.*, vol. BME-31, pp. 779–787, 1984.

[2] R. Paglione, F. Sterzer, J. Mendecki, E. Friedenthal, and C. Botstein, "RF therapy of malignancy," *IEEE Spectrum*, vol. 17, pp. 32–37, 1980.

[3] G. A. Lovisolo *et al.*, "A multifrequency water-filled waveguide applicator: Thermal dosimetry in vivo," *IEEE Trans. Microwave Theory Tech.*, vol. MTT-32, pp. 893–896, 1984.

[4] N. K. Uzunoglu, E. A. Angelikas, and P. A. Cosmidis, "A 432 MHz local hyperthermia system using an indirectly cooled, water-loaded waveguide applicator," *IEEE Trans. Microwave Theory Tech.*, vol. MTT-35, pp. 106–111, 1987.

[5] L. Lewin, *Advanced Theory of Waveguides*. London: Iliffe, 1951, ch. 6, pp. 121–144.

[6] R. T. Compton, "The admittance of aperture antennas radiating into lossy media," Rep. 1691-5, Ohio State Univ., Antenna Lab., Res. Found, Mar. 1964.

[7] V. Teodoridis, T. Sphicopoulos, and F. Gardiol, "The reflection from an open-ended rectangular waveguide terminated by a layered dielectric medium," *IEEE Trans. Microwave Theory Tech.*, vol. MTT-33, pp. 359–372, 1985.

[8] D. G. Bodnar and D. T. Paris, "New variational principle in electromagnetics," *IEEE Trans. Antennas Propagat.*, vol. AP-18, pp. 216–223, Mar. 1970.

[9] R. Antolini, G. Cerri, L. Cristoforetti, and R. De Leo, "Absorbed power distributions from single or multiple waveguide applicators during microwave hyperthermia," *Phys. Med. Biol.*, vol. 31, pp. 1005–1019, 1986.

[10] D. S. Jones, *Theory of Electromagnetism*. Oxford: Pergamon Press, 1964, ch. 5, pp. 248–251.

[11] R. V. Churchill, *Fourier Series and Boundary Value Problems*. New York: McGraw-Hill, 1941.

[12] H. P. Schwan and K. R. Foster, "RF field interactions with biological systems: Electrical properties and biophysical mechanism," *Proc. IEEE*, vol. 68, pp. 104–113, 1980.

[13] F. K. Storm, R. S. Elliott, W. H. Harrison, and D. L. Morton, "Clinical RF hyperthermia by magnetic-loop induction: A now approach to human cancer therapy," *IEEE Trans. Microwave Theory Tech.*, vol. MTT-30, pp. 1149–1158, 1982.

[14] P. F. Turner, "Mini-annular phased array for limb hyperthermia," *IEEE Trans. Microwave Theory Tech.*, vol. MTT-34, pp. 508–513, 1986.

[15] V. Sathiaseelan, M. F. E. Iskander, G. C. W. Howard, and N. M. Bleehen, "Theoretical analysis and clinical demonstration of the effect of power pattern control using the annular phased-array hyperthermia system," *IEEE Trans. Microwave Theory Tech.*, vol. MTT-34, pp. 514–519, 1986.

✠

Konstantina S. Nikita was born in Tripoli, Greece, in 1963. She received the Diploma in electrical engineering from the National Technical University of Athens, Athens, Greece, in 1986. Since 1987 she has been working towards the Ph.D. degree on the development of a four-element computer-controlled phased-array hyperthermia system. Her current research activities focus on the applications of electromagnetic waves in medicine. She is also a fourth-year student at the Medical School of the University of Athens.

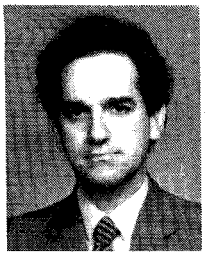

Nikolaos K. Uzunoglu (M'82) received the B.Sc. degree in electronics engineering from the Istanbul Technical University, Turkey, in 1973. He then obtained the M.Sc. and Ph.D. degrees from the University of Essex, England, in 1974 and 1976, respectively.

He worked for the Hellenic Navy Research and Technology Development Office from 1977 to 1984. During this period he also worked, on a part-time basis, at the National Technical University of Athens on electromagnetic theory. In 1984, he was elected Associate Professor at the National Technical University of Athens and in 1988 Professor, the position that he holds presently. He served as associate chairman of the Department of Electrical Engineering of the National Technical University of Athens for the years 1986–1988. In 1988 he was elected chairman of the department, a position he will hold until 1990. His research interests include microwave applications in telecommunications and medicine, fiber-optic components, and electromagnetic theory.